Chapter VI

The Electrochemical Photovoltaic (PV) Studies on $Co_{1-x}Zn_xS$ Thin Films

6.1. Introduction

Today's needs of the overall growing world are exponentially enhancing energy and the environmental concerns. Alternatives for the use of non-renewable and polluting fossil fuels have therefore to be searched out. The best alternative is the energy from the sun; available freely, free of cost, abundantly and pollution free. The solar energy is simply the energy emitted by the Sun and collected in different forms on the earth. The Sun generates energy through thermonuclear fusion process that involves conversion of hydrogen to helium; in the process a lot of energy is librated in the forms of heat and electromagnetic radiation. The majority of the heat retains at the Sun that maintains the thermonuclear reactions whereas, only a small fraction is converted into the surroundings by the converter; the Sun. The electromagnetic radiation (including visible, infra-red and ultra-violet radiation) streams out into space in all directions supplying directly the solar power, fulfilling the energy requirements of the World, which is only a fraction of the total energy produced by the Sun. Two major advantages of solar power over fossil fuels are the facts that it is completely non- polluting and available abundantly for a much longer period.

Photovoltaics (PV) is a technological approach to convert sunlight directly into electrical energy. Conceptually, in its simplest form, a photovoltaic device is a solar-powered generator, which only consumes solar radiation as a fuel. There are no moving

parts to wear out and operation is environmentally benign. As sunlight is universally available, can be used anywhere. PV has the potential to become a major energy source without affecting the global environment. In order to realize this potential, a mass production of PV modules on an industrial scale has to be technologically established which must be inexpensive, durable and efficient.

It was Edmund Becquerel (1839) who noticed first that sunlight absorbed by certain materials can produce small quantities of electricity in addition to heat. Initially, this phenomenon was limited to the use of light detectors. Then improved technological advances in material processing and the needs of the emerging space program led to the development of PV cells.

Today most of the PV cells in the market operate at an efficiency of less than 15%. Maximum theoretical efficiency for a photovoltaic cell is only 32.3% [1, 2] and at this efficiency, solar electricity is very economical. In fact most of our conventional techniques of electricity generation are less efficient than this. Unfortunately the modular efficiency is much lower than 15 %. Even though this may not be quite economical for large scale production, it is fine for indoor applications and lightings. However, hope that bulk solar electricity should not be abandoned, as very recently, solar cell with an efficiency of 28.2% has been fabricated in a laboratory [2]. About 90% of today's demand for electricity is met by the crystalline silicon solar cells as silicon semiconductor technology is fairly advanced due to its large scale application in digital/analog electronic industries. Looking to the past fifty years, although PV

technology with Si electronics has become increasingly advanced, the smaller energy band gap of Si (1.1 eV) is not ideal for PV generation and therefore attempts are being put to develop the materials with matchable electrical and optical properties for high conversion efficiency at low production and module costs. Due to advancements in silicon processing technology and availability of technical data, this material is still being used for photovoltaic conversion with increasing success.

To produce economically viable PV systems, a new approach, viz. thin film based electrochemical photovoltaic (PV) cells are gaining much popularity [3-6]. With a vast experience of almost 30 years, we hope to realize that electrochemical-PV solar cells have the potential to compete with Si-technology with a better possibility of power production at low cost. As can be seen from today's scenario, solar cell technology has been undergoing enormous developments for the last few decades, initially providing electrical power for spacecraft and recently for terrestrial systems.

The major advantage of thin film based electrochemical PV solar cells is the capability to produce electric power at low cost [3-6]. This is mainly because these types of cells require low quantity of materials even when they use large area. Moreover, large scale fabrication is feasible. Different types of techniques available for thin film depositions make them possible to fabricate new compound semiconductors for better thin film based PV-devices and this is a unique forte of Thin Film Science. Presently, thorough intensive research work, three semiconducting materials have been identified for large scale production of thin film solar cells. They are the amorphous silicon, cadmium

telluride and copper indium selenide [6-7]. Amorphous Si has recently achieved an efficiency of l3.5% [3], however, radiation induced defects (Stabler-Wronsky defect) formation reduces the efficiency during continuous illumination. CdTe based PV cells have reached a maximum efficiency of 16 %. The problems associated with this type of cell are the lack of completely optimized manufacturing set up and those related to the stability of cell and use of poisonous cadmium and tellurium [7, 8]. $Cu(In,Ga)Se_2$ based solar cells have achieved the best efficiency of more than 18%,which required an extensive research in CIS based cells by several groups all over the world [9]. However, it remained yet to produce large area films at low cost using ecofriendly technique.

In the present work, we describe our firm efforts to fabricate $Co_{1-x}Zn_xS$ thin films via a low cost, simple and eco-friendly chemical solution technique and to employ them in electrochemical PV cells. The most imperative advantage of the proposed technique is that, the method avoids engrossment of poisonous gases. Instead, thin film deposition is achieved at mere expense of chemical reaction between the aqueous solutions resulting in both binary and ternary yields.

6.2. The Fundamentals of an Electrode / Electrolyte Interface

In recent years, semiconductor-electrolyte based PV-cells are attracting a great deal of interest in the field of solar energy conversion [3, 4-7, 10]. They are simple to devise compared to conventional p-n junctions or Schottky barrier cells, which require highly pure semiconductor materials prepared under stringent controlling conditions. The conversion efficiencies of these cells are comparable to those obtained from

conventional solid state photovoltaic devices. These devices have an additional inherent advantage that either electricity or useful chemical energy with potential applications can be produced at the interface whereas only direct electricity generation occurs with solid state counterpart. Photoelectrode immersed in the electrolyte and upon exposure to sunlight, converts solar radiation into electrical energy by creating delocalized charges with high yield. The electron-hole pairs give the redox species and the charge transfer process across a photoelectrode-electrolyte interface (in dark or in light) results in the net current flow through the junction.

To begin with the study of electrochemical PV cell, we must examine the energy level diagram of the photoelectrode and an electrolyte. The simple electrochemical PV cell consists of a semiconductor electrode dipped into an appropriate electrolyte to form a junction to be illuminated by a suitable light. When an n-type semiconductor having energy gap E_g is immersed in a matchable electrolyte, the electrochemical potential of the electrons in semiconductor electrode is represented by its Fermi energy level, while for liquid electrolyte, the electrochemical potential is represented by the $E_{F,\,redox}$.

A redox couple implies two electro-active species in the solution, one being an electron donor and other an acceptor. The transfer of electric charge across the electrode/electrolyte interface produces a region on each side of the junction where the charge distribution differs from bulk of the materials and this is known as space-charge layer. This layer provides the initial Fermi levels of the two phases which are different. When the electrode is immersed in an electrolyte, electron transfer takes place at the

interface until the Fermi levels equilibrate; electrons from the electrode are transferred to the solution that makes electrode positively charged. These charges (positive on the electrode side and –ve on the solution side) are distributed in the space-charge region near the surface. The valence and conduction band edges bend as a result of the formation of space charge region, establishing a potential barrier against further transfer of electrons into electrolyte. The direction of the field is such that the holes generated in the space charge region (upon illumination) move towards the interface while excess electrons move towards the bulk of the semiconductor. The width of the space charge is given by [3, 4, 6, 10];

$$W = \left(2\varepsilon_s \varepsilon_0 V_B \Big/ eN_D \right)^{1/2} \qquad \text{.....(6.1)}$$

where, V_B is the extent of band bending in the depletion layer, e is an electronic charge, N_D is the donor density in the photoelectrode, ε_s is the dielectric constant of the photoelectrode material and ε_0 is the permittivity of the free space.

Similarly, a negatively charged layer (Helmholtz layer) also exists on the solution side of the interface, which is made up of ions that are charged opposite to the charge in the depletion region. The width of the Helmholtz layer is of the order of a few Å.

The energy levels of the photoelectrode and electrolyte are related via a parameter known as the flat band potential (V_{fb}). It is the electrode potential applied externally to the photoelectrode at which the conduction and valence bands become flat. V_{fb} is influenced by the specific adsorption of the ions from the electrolyte on the surface of

the photoelectrode. At equilibrium (in dark) the electrode potential (E_F) is equivalent to the potential of redox couple (V_{redox}). The extent of band bending is then given by,

$$V_b = V_{redox} - V_{fb} . \quad \text{.....(6.2)}$$

This is the driving force for the separation of electron-hole pairs when an electrode/electrolyte interface is illuminated by the light.

When the photons of energies greater than E_g are absorbed in the semiconductor, electron-hole pairs are generated, which are separated by the electric field at the space charge. The minority carriers (holes for n-type) move towards the semiconductor-electrolyte interface and produce an anodic oxidation reaction. The majority carriers (electron for n-type) move towards the semiconductor bulk constituting an electric current through the external circuit and subsequently produce a cathodic reduction reaction at the counter electrode. The possible reactions in addition to recombination after the absorption of light are [3, 4, 10];

$$p^+(\text{photoelectrode surface}) \rightarrow R \rightarrow O \quad \text{.....(6.3)}$$

$$e^-(space\ ch\arg e) \rightarrow e^-(bulk) \quad \text{.....(6.4)}$$

And/or

$$p^+ + \text{photoelectrode} \rightarrow \text{decomposition of the photoelectrode} . \quad \text{.....(6.5)}$$

It is evident that stability of the photoelectrode in electrochemical PV- cells depends directly on the minimization of the reaction (6.5) and at present, it seems to be bottleneck in efficient conversion of solar energy.

When the photoelectrode is immersed in an electrolyte, it acquires a charge density. The photoelectrode becomes positively charged compared to the solution due to the loss of the electrons. These electron enters into the electrolyte decreasing the total cation concentration. At the interface, an electrical double layer consisting of a sheet of the positive charges at the surface of the electrode and a sheet of the negative charges in the solution or vice versa is formed. The overall charge neutrality occurs when

$$q_s = q_l \qquad \text{.....(6.6)}$$

where, q_s and q_l are the charges on the semiconductor and an electrolyte sides of the interface, respectively. This interface can be classified into two; an electrolyte side of the interface and the semiconductor side of the interface

6.2.1. An electrolyte side of the interface

Helmholtz [3, 4, 10] assumed that the charged layer of the ions form a sheath at the dipped side of the photoelectrode surface. The model suggests that the electrode/electrolyte interface is similar to the parallel plates of a condenser, charged oppositely. The term ‘double layer’ thus originates and almost all the potential is assumed to be dropped across this double layer of width δH. Gouy and Chapman suggested that the electrode surface on which charges have accumulated may be considered as large central ion exerting a planar electrostatic field on solution side of the interface. The differential capacitance of layer is dependent on the voltage applied to it and electrolyte concentration. The diffused layer is known as Gouy layer. The force falls off slowly as we move deep into the bulk solution. Stern noted that the ions being of

finite size, keep minimum distance of approach to the electrode surface. Thus, a layer is neither abrupt nor diffused but combination of the two. The situation is as shown in fig. 6.1.

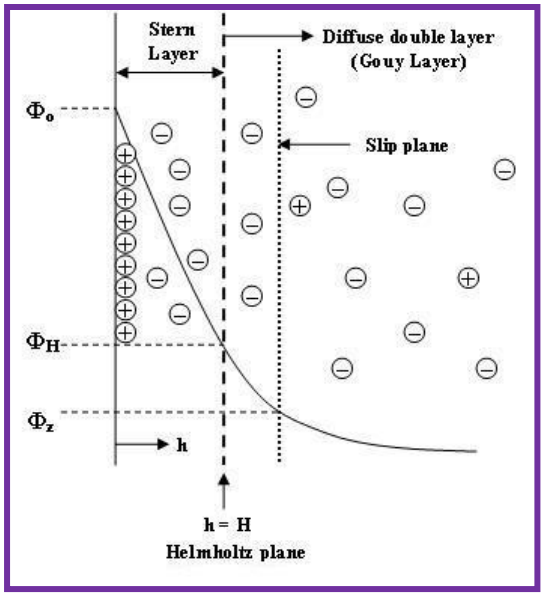

Figure 6.1. A semiconductor-electrolyte interface (Stern model).

According to Stern, the interface distribution is divided into two layers such as dense layer & diffused layer. In dense layer, the ions stick to the electrode and potential variation is linear, whereas a diffused layer is formed as a result of opposing tendencies of attractive columbic force and discarding thermal fluctuations, where the potential decays exponentially, as shown in fig. 6.1. The Stern model does not explain explicitly how the ions adhere to the electrode. The probable reason may be due to hydrated electrode surface and "stripping off" the solution. This means pushing some water molecules away so that the ion can come in close contact with the electrode. The ions so 'sitting' are called "contact adsorbed ions" and locus of all such contact adsorbed ions

forms the inner Helmholtz plane (IHP). The solvated ions are in the outer Helmholtz plane (OHP) as shown in fig. 6.2.

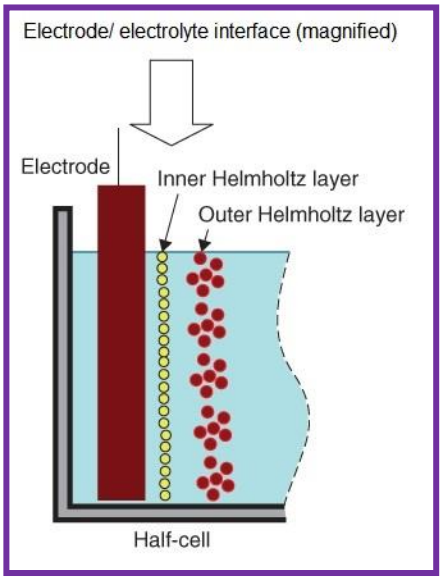

Figure 6.2. Magnified electrode/electrolyte interface highlighting Helmholtz layer.

The IHP consisting of water dipoles and adsorbed ions, forms a dense sheet near the electrode surface. The OHP consisting of solvated ions at a distance of their closest approach to the electrode surface, hence OHP consists of partially orientated water molecules. The region with IHP and OHP constitutes the compact part of Helmholtz double layer. The specific adsorption of ion, which is responsible for formation of a layer, is controlled by the nature of ions in solution as well as the nature of the electrode material and potential applied to it. This observation is correct at low ion concentration. At higher concentration, the screening charge cloud assumes a layered structure. Liu [11] has developed a lattice gas model suggesting the ions and solvent molecules as the hard spheres of almost equal radii forming parallel layers near the planar electrode. The

lattice parameter is chosen as the distance of closest approach of the two molecules. Liu's model gives a reasonable description of the properties of electrolyte in the interface region and is better than all the other approaches [3, 4].

6.2.2. The electrode side of the interface

Systemic investigations on the electrode/electrolyte interface has been given by Chandra et al. [3, 4, 10, 12]. The rearrangement of electrons and ions at the interface are due to anisotropic forces at the electrode/electrolyte interface and charge transfer across the interface. The charge distribution across the metal and semiconductor junction are different because;

i) There are two types of charge carriers (electrons and holes) in semiconductors but in metals electrons are the only charge carriers.

ii) The charge carrier density in semiconductor is of the order of 10^{16} to 10^{19} /cm^3 while in the metals it is 10^{28} to 10^{32} /cm^3.

iii) For metals, the charge carriers are at the surface, while for semiconductor they form a space charge layer within the semiconductor near the interface.

On the semiconductor side of the junction, the nature of the band bending depends on the position of the Fermi level in the solid. If the Fermi level of the electrode is equal to the flat band potential, there is no excess charge on either side of the junction and the bands are flat. If electrons accumulate at the semiconductor side, one obtains an accumulation layer. Such a layer leads to downward bending of the bands for an n-type semiconductor and upward for a p-type semiconductor. If the surface becomes depleted

of the majority charge carriers then space charge layer is formed called as depletion layer. If the charge distribution is such that the minority charge carriers concentrate at the surface greater than that of bulk, the space charge layer is called an inversion layer, which leads to a large upward band bending in n-type and downward band bending in p-type semiconductors. Fig.6.3 illustrates an n-type semiconductor where electrons are the mobile charge carriers.

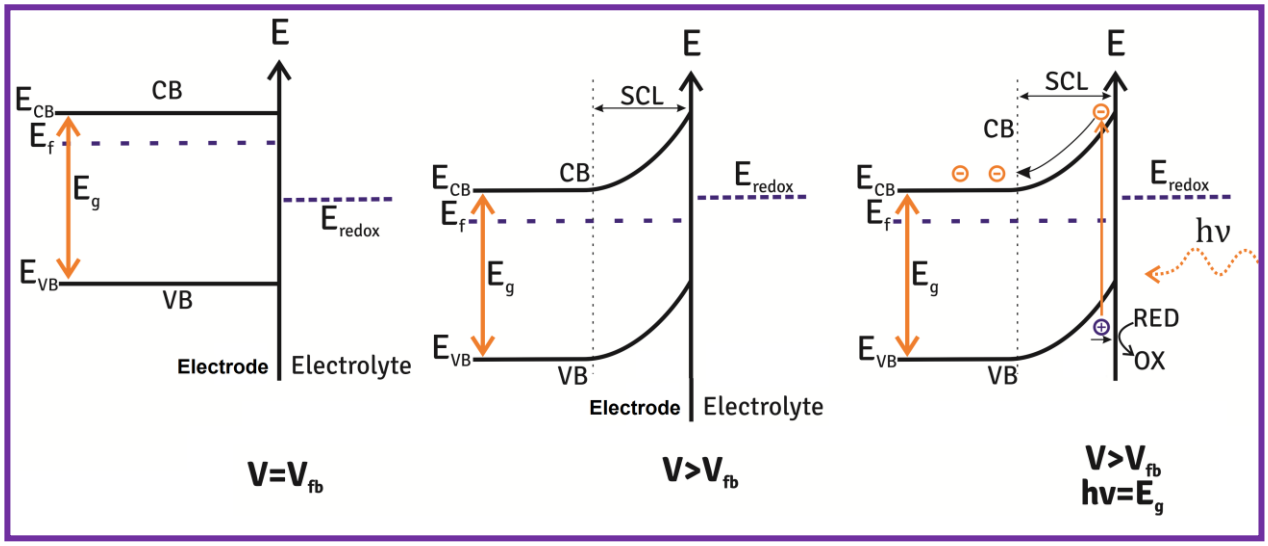

Figure 6.3. Energy band diagram for an n-type semiconductor before and after the equilibration of Fermi levels at the interface and the appearance of band-bending and the space charge layer (SCL).

6.2.3. The surface states and surface adsorbed ions

The potential and the charge distribution at the electrode-electrolyte interface are affected by the surface states and surface adsorbed ions [3, 4, 10, 12]. The surface states are essentially the result of non-periodicity of the lattices at the boundary, which lead to the formation of electronic states localized at the interface. The adsorption of foreign

atoms or ions can also generate the surface states. The resulting model of an electrode-electrolyte interface consists of: i) diffused charged layer in the semiconductor indicating surface states and surface adsorbed ions, ii) Helmholtz layer and iii) Gouy layer. The surface states are roughly classified into two groups: a) short relaxation time: 10^{-3} down to 10^{-6} s (intrinsic) and b) long relaxation time: 1s (extrinsic). The surface states can be made to populate or depopulate by changing the electrode potential. Due to the presence of surface states, a layer of depleted conductivity is formed below the surface. Under these circumstances, the space charge layer is a property of the material itself and not particularly sensitive to work function, which may be brought in contact with the surface. The presence of surface states also plays a role in the interpretation of contact potential measurements across a p-n junction [3, 4, 10, 12].

6.2.4. The differential capacitance and Mott-Schottky plots

Neglecting the contribution from surface states and the surface adsorption as a first approximation, the simplest electrical equivalent of a semiconductor-electrolyte interface can be considered as the series combination of the capacitance due to three layers [space charge capacitance (C_{SC}), Helmholtz capacitance (C_H) and Gouy layer capacitance (C_G)]. Hence, the total capacitance (C_T) is given by [3, 4, 10, 12],

$$1/ (C_T) = 1/ C_{SC} + 1/ C_H + 1/ C_G \, . \qquad \text{.....(6.7)}$$

For moderately concentrated electrolytes, the value of Helmholtz capacitance and Gouy layer capacitance can be neglected, as a result, the capacitance is only due to the space

charge layer. A model to account for behaviour of the surface states can be incorporated into an equivalent circuit of the interface as shown in fig. 6.4.

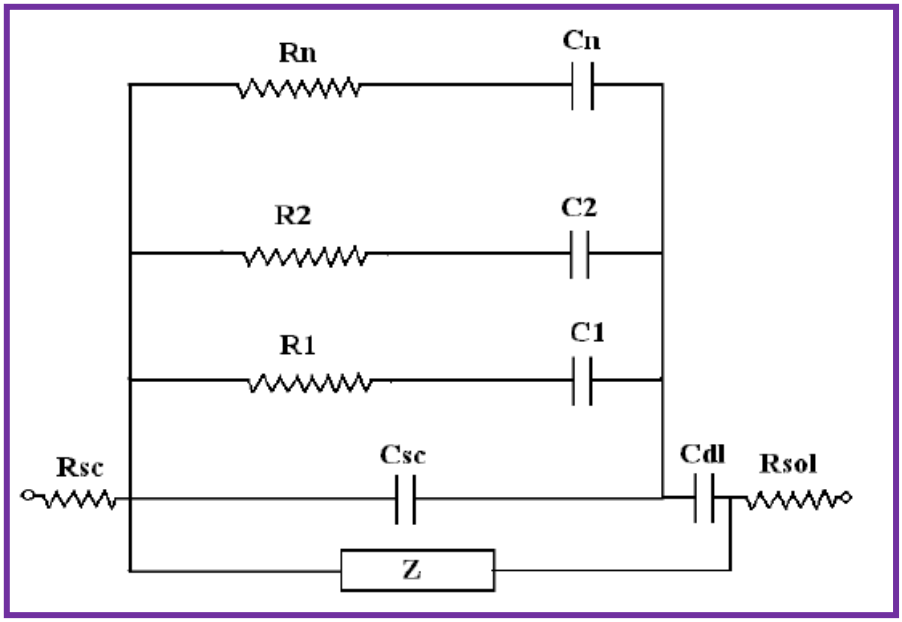

Figure 6.4. An equivalent circuit diagram for semiconductor-electrolyte interface showing the presence of surface states and surface adsorbed ions.

Each of the surface states is represented as a series combination of a capacitance (C) and a resistance (R). The surface states are in parallel with each other and with the semiconductor space charge capacitance (C_{SC}). The total capacitance of the electrode is therefore, $C_{SC} = \sum C_T$ .This network of parallel capacitances is in series with the bulk resistance (R_s) of the photoelectrode material, the double layer capacitance (C_{dl}) and the solution resistance (R_{sol}) between the semiconductor and reference electrode.

The Faradic process, if any, short across C_{SC} and C_{dl} as represented by Z. The double layer capacitance is far greater than C_{SC} i.e. $C_{dl} >> C_{SC}$ and hence can be ignored. Thus,

the measurement of differential space charge layer capacitance provides an important and convenient tool to analyze the electrode-electrolyte interface. Neglecting the effects due to the surface states and assuming high ionic concentration of the redox couple and fully ionized nature of the donors and the acceptors, the space charge layer capacitance is given by [3, 4, 10, 12];

$$1/C_{SC}^2 = (2/\varepsilon_s\varepsilon_0 qN_D)\,(V-V_{fb}-KT/q) \qquad \text{.....(6.8)}$$

where, ε_s is the dielectric constant of the photoelectrode material, ε_0 permittivity of free space, N_D is the donor concentration, V is the applied electrode potential and V_{fb} is the flat band potential. The above equation is a famous Mott-Schottky equation according to which a plot of $1/C_{SC}^2$ versus V should be a straight line intersecting on voltage axis giving the flat band potential (V_{fb}) and slope of line gives donor concentration. The Mott- Schottky plot determines the type of majority carriers and the band bending, V_b, which is maximum open circuit voltage attainable from a PV- device. The V_b is related to V_{fb} as;

$$V_b = [(E_{f,\,redox}/q)-V] \qquad \text{.....(6.9)}$$

where, $E_{f,\,redox} = (4.5\ V_{NHE} + qV_{redox})$. .....(6.10)

The depletion layer width (W) and the position of the band edge can be determined from the equation,

$$W = (2\ \varepsilon_s\varepsilon_0/qN_D)\,(V-V_{fb}-KT/q)^{1/2} \ . \qquad \text{.....(6.11)}$$

The Mott-Schottky behaviour is an ideal behaviour for an electrode-electrolyte interface. The deviation from an ideal behaviour of the interface is due to the following reasons [3, 4, 10, 12];

1) Geometrical factors such as the edge effect, non-planar interface, surface roughness, etc.
2) Non-uniform doping.
3) Presence of both donor and acceptor impurities.
4) Presence of deep donor and acceptor levels.
5) An extra contribution to the total capacitance due to: a) presence of an oxide film, b) Helmholtz layer capacitance, c) ionic adsorption on the surface and d) acid-base equilibrium at the interface.

The presence of surface states gives complicated structure of the Mott-Schottky plots, since they exchange carrier with either of bands or to both by electrostatic coupling.

6.2.5. The charge transfer mechanism across the photoelectrode-electrolyte interface

a) Under illumination

When a semiconductor-electrolyte interface is illuminated the electron-hole pairs are generated in the depletion region and are separated by an electric field at the interface [3, 4]. This charge separation process results in generation of a counter field, which is maximum at the open circuit condition and is indicated by V_{oc}. This photovoltage acts as driving force for electrons to move from the semiconductor to counter electrode,

whereas the holes are captured by reduced species in electrolyte to undergo oxidation reaction. The whole redox reaction can be written as;

$$\text{Red (solv)} + h^+ \rightarrow \text{Ox (solv)}, \qquad \text{(at semiconductor electrode)} \qquad \text{.....(6.12)}$$

$$\text{Ox (solv)} + e^- \rightarrow \text{Red (Solv)}, \qquad \text{(at counter electrode).} \qquad \text{.....(6.13)}$$

The electrode acts as a shuttle in charge transfer process. The quasi-Fermi levels for electron (E_{fn}) and for hole (E_{fp}) in the depletion region are assumed to be flat. If U is the separation between them then [3, 4, 10, 12];

$$qU = E_{fn} - E_{fp} \qquad \text{.....(6.14)}$$

It is believed that U > V because minority carrier concentration under illumination is larger than its concentration in dark. For holes to flow from semiconductor surface to the electrolyte, U is defined as;

$$[\exp (qU/kT)] = P(w)/P_0 \qquad \text{.....(6.15)}$$

where, P(w) is the hole concentration at the edge of the depletion region and P_o is the equilibrium hole concentration in the bulk of the semiconductor in dark. It is assumed that most of the applied voltage appears across the semiconductor depletion region. Thus the series resistance of a cell should be negligible and an electrolyte concentration should be high enough such that $C_H >> C_{sc}$. The depletion layer width (W) under these conditions is given by;

$$W = W_o\ (V_D - V_o)^{1/2} \qquad \text{.....(6.16)}$$

where, $W_o = [2\varepsilon_s\varepsilon_o/q.N_D]$ and ε_s is the dielectric constant of the material and ε_o is the

permittivity of the free space, N_D is the donor concentration and V_D is the equilibrium band bending voltage.

If S_t be the surface transfer velocity, S_r is the surface recombination velocity, Φ is the incident photon flux after allowing the losses due to reflection and absorption by the electrolyte, α be the light absorption co-efficient and W is the width of the depletion region, the minority carrier flux due to hole injection can be given by,

$$J = (S_t/S_r)\,\Phi\{[1-\exp[(\alpha\text{-w})/(1+\alpha t)]\}. \qquad \text{.....(6.17)}$$

The direction of this generated photocurrent is from the semiconductor electrode to the electrolyte [4, 12].

b) In dark

Under suitable values of the valence and conduction band edges and redox energies, the charge may be transferred from an electrolyte to the semiconductor or vice versa. The ionic species will be reduced or oxidized at the respective electrode. They can also jump back in the reverse directions so that there can occur oxidation and reduction. If a positive ion moves against the field direction in a reduction reaction, it will move in the direction of field in oxidation. This is shown in fig. 6.5. If the positive ion is to be activated through a potential difference, βΔΦ, in reduction reaction, then it has to be activated by (1- βΔΦ) in oxidation, where β is the symmetry factor and Φ is a potential through which an ion passes. The net current density can be given by the Butler-Volmer equation [3, 4, 10, 12];

$$I = I_o\{\exp[(1-\beta)\,V_F/RT] - \exp(-\beta V_F/RT). \qquad \text{.....(6.18)}$$

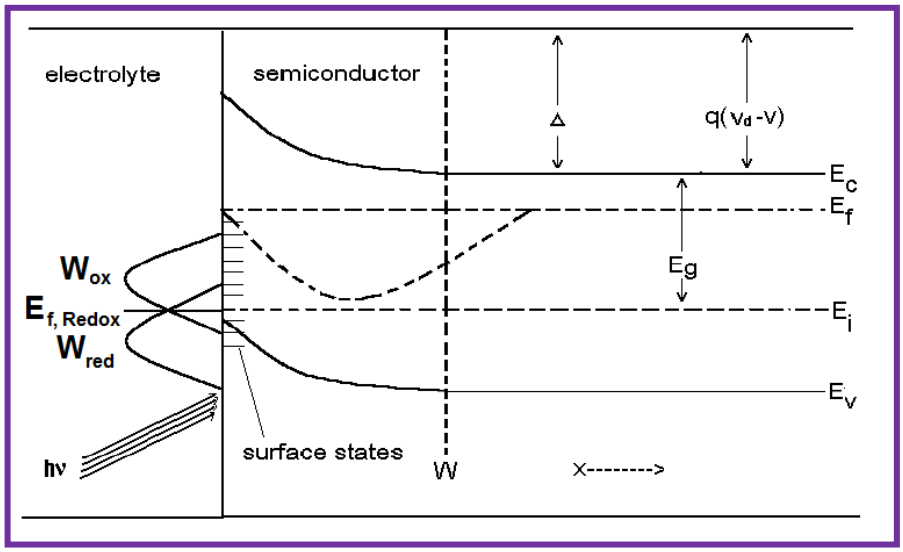

Figure 6.5. An electron energy level diagram for n-S/E interface under illumination and biasing voltage 'V'.

The above equation shows the dependence of current density across the interface on the potential V_F. A small variation in V_F produces a large change in current density. In the electrode-electrolyte system, a hill shaped potential barrier is present even in the absence of electric field. This barrier is related to the atomic movements during bond stretching, which is prerequisite for processes such as chemical reaction and the diffusion of atoms / ions. The electric field modifies the existing potential barrier such that only a fraction (1-β) of the input electrical energy (qV) turns into activation energy and hence in the rate expression. This is because the atomic movements necessary for the system to reach a barrier peak is only a fraction of the total distance over which the potential barrier extends.

6.2.6. The cell efficiency (η)

The ratio of the maximum output power to the input power is called as conversion

efficiency.

$$\eta\% = \frac{\text{Maximum power output x 100}}{\text{Input power}}. \qquad \text{.....(6.19)}$$

From the input power source, the photon energy less than the band gap of the semiconductor electrode is not absorbed. The photons having energies higher than the band gap are useful for the generation of electron-hole pairs in an electrochemical PV-cell. The conversion efficiency (η) is given by [3, 4, 10, 12];

$$\eta = \frac{\text{Eg} \int_0^\infty \alpha\ (\text{E}).\text{E}.\text{N}(\text{E})\ d\text{E}}{\int_0^\infty N(E)dE} \qquad \text{.....(6.20)}$$

where, E_g is the band gap, α(E) is the fraction of photon absorbed, N (E) is the number of photons incident having energy E. The various factors such as ohmic losses, light absorption in the solution etc, are neglected. The above equation suggests that, if a value of band gap as well as absorption coefficient is high, the efficiency will be higher. α (E) near the band edge is approximated as,

$$\alpha\ (\text{E}) = \text{A}\ (\text{h}\nu\text{-E}_\text{g})^\text{n}/\text{h}\nu \qquad \text{.....(6.21)}$$

where, A is a constant, n = ½ suggests the type of transition as allowed direct type. In order to obtain higher α (E), the E_g should be small. This leads to the contradiction. Hence efficiency should be maximum at some optimum value of E_g (≈ 1.2 - 1.4 eV). In addition to Eg, there are some other factors which affect the efficiency of PV cells and these can be summarized as below [3, 4, 10, 12];

1) Physical properties of the semiconductor,

2) Energy losses due to the photo-induced redox reactions,
3) Light losses due to absorption in the electrolyte, reflection from the semiconductor surface, etc.
4) Ohmic losses due to the resistance of the electrolyte, semiconductor, etc.
5) Losses due to concentration polarization if the redox process is slow.

Both condition (4) and (5) can be minimized by keeping the distance between the counter electrode and the photoelectrode to a minimum extent. Further, electrolyte stirring may also help in reducing the concentration polarization by facilitating better transport of the redox species to the respective electrodes. A transparent electrolyte would be preferable to avoid light absorption in the electrolyte. Considerations such as 3 and 5 further impose restrictions on the choice of E_g. Further, the net energy available should be sufficient to overcome the losses as well as to be able to drive the redox reactions i.e. $h\nu = E_g$ = energy required to drive the redox reaction + losses due to over potential, ohmic resistance, etc.

Another parameter called fill factor (ff) is defined as;

$$ff\,\% = \frac{\text{Maximum power output}}{V_{oc} I_{sc}} \qquad \text{.....(6.22)}$$

where, V_{oc} and I_{sc} are the open circuit voltage and short circuit current, respectively. The fill factor must be high to extract more power from a PV-cell. The maximum open circuit voltage attainable from an electrochemical PV-cell would be,

$$V_{oc} = V_{redox} - V_{fb}\,. \qquad \text{.....(6.23)}$$

Thus efficiency also depends upon V_{redox}.

6.3. Experimental Details

6.3.1. Deposition of the samples

CoS and $Co_{1-x}Zn_xS$ thin films were synthesized onto the well-polished stainless steel substrates from an alkaline bath as described earlier (section 2.3) [14-16]. The film composition was varied by varying the volume concentrations of Co^{2+} and Zn^{2+} ions in the reaction bath. The reaction was allowed for 90 min at a pH value of 9.0 ± 0.1. The polished and cleaned stainless steel substrates mounted on a specially designed substrate holder were kept rotating at 65 ± 2 rpm speed in the reaction bath. The deposition temperature was controlled to its optimized value (80 ± 0.5°C). A detailed account of the deposition process is described elsewhere (chapter 3).

6.3.2 Fabrication of the semiconductor/electrolyte junction PV-cell

A semiconductor/ electrolyte junction PV-cell is fabricated and consists of two test tubes. The H-shaped assembly was formed by coupling test tubes using a small capillary tube. This H-shaped assembly was fitted in a copper vessel of suitable size. A window of the suitable dimension was made for illumination of the electrode material. A PV cell of the configuration $Co_{1-x}Zn_xS$ /electrolyte/C was then devised with a sensitized graphite rod. The active area of the sample was exposed to light. The detailed fabrication of an electrochemical PV- cell is given in chapter II (Section 2.5.2).

6.3.3. On the electrolyte selection

The match of an electrolyte redox couple, being an important consideration, was tackled through the various electrolyte studies. These electrolytes were prepared in double

distilled water and used at spot.

a) Sulfide/ polysulfide electrolyte

1M sodium sulfide was triturated with 1M sulphur powder and was dissolved in an appropriate quantity of double distilled water. To this, 1M NaOH was added and resulting solution was stirred and stored in an air sealed bottle.

b) Ferri / Ferrocynide

1M potassium ferrocynide and 1M potassium ferricyanide were mixed together to form a ferri / ferrocynide electrolyte couple.

c) Dimethyl Sulfoxide

1 M dimethyl sulfoxide solution was taken directly as an electrolyte.

d) Iodite / Polyiodite

1M sodium iodite was mixed with iodine crystals dissolved in double distilled water.

e) Ammonium chloride (NH_4Cl)

1M ammonium chloride was dissolved in distilled water and was used as an electrolyte.

f) Sulphuric acid (H_2SO_4)

1M sulphuric acid solution was taken directly as an electrolyte.

g) Hydroquinone

0.5M hydroquinone dissolved in distilled water was used as an electrolyte.

h) Potassium chloride (KCl)

1M potassium chloride was dissolved in distilled water and was used as an electrolyte. The electrochemical PV- cells were fabricated with CoS/ $Co_{1-x}Zn_xS$/ C thin films as a

photoelectrode, electrolyte redox couple and a sensitized graphite rod as a counter electrode. The I_{sc} and V_{oc} were measured as usual.

6.3.4. Characterization of the electrochemical photovoltaic (PV) cells

The photovoltaic effect was studied for both pure CoS and $Co_{1-x}Zn_xS$ materials by forming a semiconductor / liquid junction rectifying contacts obtained by dipping the semiconductor electrode in an electrolyte. A sensitized graphite rod (in cobalt sulfide for about 24 hrs) was used as a counter electrode. The fabrication and schematic given in section 2.5.2 were used to record the observations on the following properties:

a) The electrical properties

The mechanism of charge transfer process across the electrode / electrolyte interface was examined by the studies on electrical properties of the PV- cells. These properties comprise I-V and C-V characteristics in dark, measurement of built-in-potential and power output characteristics under illumination. A potentiometric arrangement was used to study the I-V characteristics in dark and power output characteristics in light (section 2.5.3). To compute the built-in-potentials, reverse saturation currents of the various cells was measured as a function of the cell temperature. The input light intensity for the power output measurements were 25 mW/cm^2 and was measured with a LX-101 Lutron (Taiwan) lux meter.

b) The optical properties

The optical properties namely, photo response, spectral response and transient response were studied for various cell configurations. The short circuit current (I_{sc}) and open

circuit voltage (V_{oc}) were measured at different illuminations from 5 mW/cm^2 to 50 mW/cm^2. The short circuit current (I_{sc}) was also measured as a function of the incident wavelengths (350 nm to 1250 nm) to study the spectral response. The rise and decay of the photocurrent was also measured. The detailed procedure is given in the section 2.5.4.

6.4. Results and Discussion

The scientific scenario of the solar cells has been dominated by inorganic solid-state material devices, especially doped forms of crystalline and amorphous silicon. However, this dominance is now being challenged by the emergence of new generation devices based on polycrystalline materials. In the present power-crisis, scientific community is motivated towards the development of alternative novel materials including those related to the economic as well as to health and environmental concerns. In view of this, solar energy conversion utilizing electrochemical photovoltaics has been considered as the most intensive approach and is employed in the fields of photoelectrolysis, photocatalysis and electrochemical storage devices [17-23]. The direct conversion of solar energy into electrical using semiconductor/electrolyte junction was first demonstrated four decades back. Since then a large number of sulphide semiconductors as well as mixed chalcogenide and oxides have been used as the photoelectrode materials in electrochemical PV cells. The stability and efficiency of these cells are mainly dependent on the electrode preparation conditions, properties of an electrolyte and the experimental conditions set during the experiment [14-23]. The basic requirements of a good thin film photoelectrode for electrochemical PV-cells are the low

resistivity and larger grain size. Large grain size leads to reduction of grain boundary area of the thin film leading to an efficient energy conversion. The low resistivity of the photoelectrode material is required to minimize the series resistance of the PV- cell, which leads to enhance the short circuit current [3, 4, 10, 12, 17]. These cells provide an economical chemical route for trapping solar energy and consists of a photosensitive n or p-type semiconductor electrode and a counter electrode dipped in a suitable electrolyte. Charge transfer leads to an equilibrium condition and corresponding potential difference is developed in both phases.

A Schottky barrier with a space charge ionized donor or acceptor ions is formed within the semiconductor and the minority carriers are present in too low concentration. Upon illumination of this interface with a light of suitable wavelength, electron-hole pairs are generated and separated by a barrier at the interface; holes arrive at electrode surface whereas the electrons are driven into the semiconductor. Under short-circuit condition, current is proportional to the intensity of the incident light whereas at the open circuit condition these electrons and holes do not recombine. For an efficient conversion of incident light into electrical energy, an ohmic contact between the photoelectrode material and the substrate is of importance. A contact is said to be ohmic, if it is non-injecting and has a linear current-voltage relation in both directions [12]. Therefore, nature of the contact between the photoelectrode and the substrate was examined for both types of samples.

6.4.1. The choice of an electrolyte system

An electrolyte is ionically bonded substance, which dissociates in a solvent and increases ionic conductivity of the solution or acts as a conductor between two dissimilar metals in a battery or a galvanic couple. The role of an electrolyte is thus crucial in PV-cells and is customary to find out a satisfactory match of a specific photoelectrode material and an electrolyte. The various electrolyte systems used in the studies were; 1) Sulfide /polysulfide, 2) Iodite / polyiodite, 3) Ferri / ferrocynide, 4) Dimethyl sulphoxide (DMSO), 5) Sulphuric acid (H_2SO_4), 6) Ammonium chloride (NH_4Cl), 7) Hydroquinone and 8) Potassium chloride (KCl).

These electrolyte systems were freshly prepared in double distilled water and various electrochemical PV-cells were then fabricated. For each of the cells, the open circuit voltage (V_{oc}) and short circuit current (I_{sc}) were measured for different electrolyte concentrations (0.25 M, 0.5 M, 1 M and 1.5 M). The V_{oc} and I_{sc} values are documented in the table 6.1. It is found that potassium chloride (0.5 M, KCl) electrolyte system has relatively better match with both the CoS and $Co_{1-x}Zn_xS$ electrodes.

6.4.2 Studies on the electrical properties of the PV cell

For electrochemical PV-studies, various PV-cells were formed with these electrodes. The electrical properties namely, I-V and C-V characteristics in dark and power output characteristics under constant illumination were studied. The barrier heights at the interfaces of these cell configurations were also determined.

a) I-V characteristics in dark

Current-Voltage (I-V) characteristics of the various electrochemical PV cell were studied at 303 K. The dark voltages and dark currents were noticed. The polarity of dark voltage was negative towards the semiconductor electrode. The dark voltage is developed due to difference between the two half-cell potential of a cell and can be expressed as;

$$E = E_{Co_{1-x}Zn_xS} - E_{Graphite} \quad \text{.....(6.24)}$$

where, $E_{Co_{1-x}Zn_xS}$ and $E_{Graphite}$ are respectively the half-cell potentials developed when $Co_{1-x}Zn_xS$ and graphite electrodes are dipped into electrolyte. From the observed polarity it is seen that,

$$E_{Co_{1-x}Zn_xS} < E_{Graphite}\,. \quad \text{.....(6.25)}$$

After illumination of the junction, the magnitude of the voltage increased and remained steady and semiconductor become more and more negative indicating electrodes to be of n-type.

Our thermopower measurements also showed n-type polarity of these materials. Existence of dark current shows that there is some deterioration of the photoelectrode materials in the electrolyte [3-6, 12]. Considering semiconductor/ electrolyte interface as the analog of a Schottky barrier cell, the current transport through the interface is defined by a Butler-Volmer relation as [3-5, 10, 12];

$$I=I_0\left\{e^{(1-\beta)V_F/RT} - e^{-\beta V_F/RT}\right\} \quad \text{.....(6.26)}$$

where, I_o is the equilibrium exchange current density, V is the over voltage, β is a symmetry factor, F is a Faraday constant and R is an universal gas constant. A value of β equal to 0.5 indicates presence of a symmetrical barrier which results in a symmetrical I versus V curves. If $\beta \neq 0.5$, the curves would be asymmetrical (our case) and the interface has rectifying properties called as Faradic rectification. The characteristics are non-symmetrical indicating the formation of rectifying type junction [4-6, 12, 22].

In the present investigation, β is found to be greater than 0.5 for all the cells suggesting the rectifying nature of the interface [33]. The dynamic current-voltage characteristics are shown in fig. 6.6. From the studies it appeared that the magnitudes of steady state current and voltages developed in dark for all the cells were found to be higher (expected to be much lower, ideally zero). This indicates that quality of our samples is not that much smooth (supported by AFM studies). Samples are porous that allows shunting paths through the material that increases the dark current. Voltages are also higher compared to our earlier studies. The junction ideality factors (n_d's) were then determined for all the cells from the plots of log I vs V and the variations are shown in fig.6.7. Linear regions of the plots were used for the estimation of junction ideality factors. The higher values of n_d suggest the dominance of series resistance as well as the structural imperfections induced by addition of Zn in CoS lattice. Defect levels introduced in this manner inside the valence band and energy gap acts as carrier traps or recombination centers. The junction ideality factor has a smaller value for x = 0.15 suggesting lowest trap density at the photoelectrode-electrolyte interface.

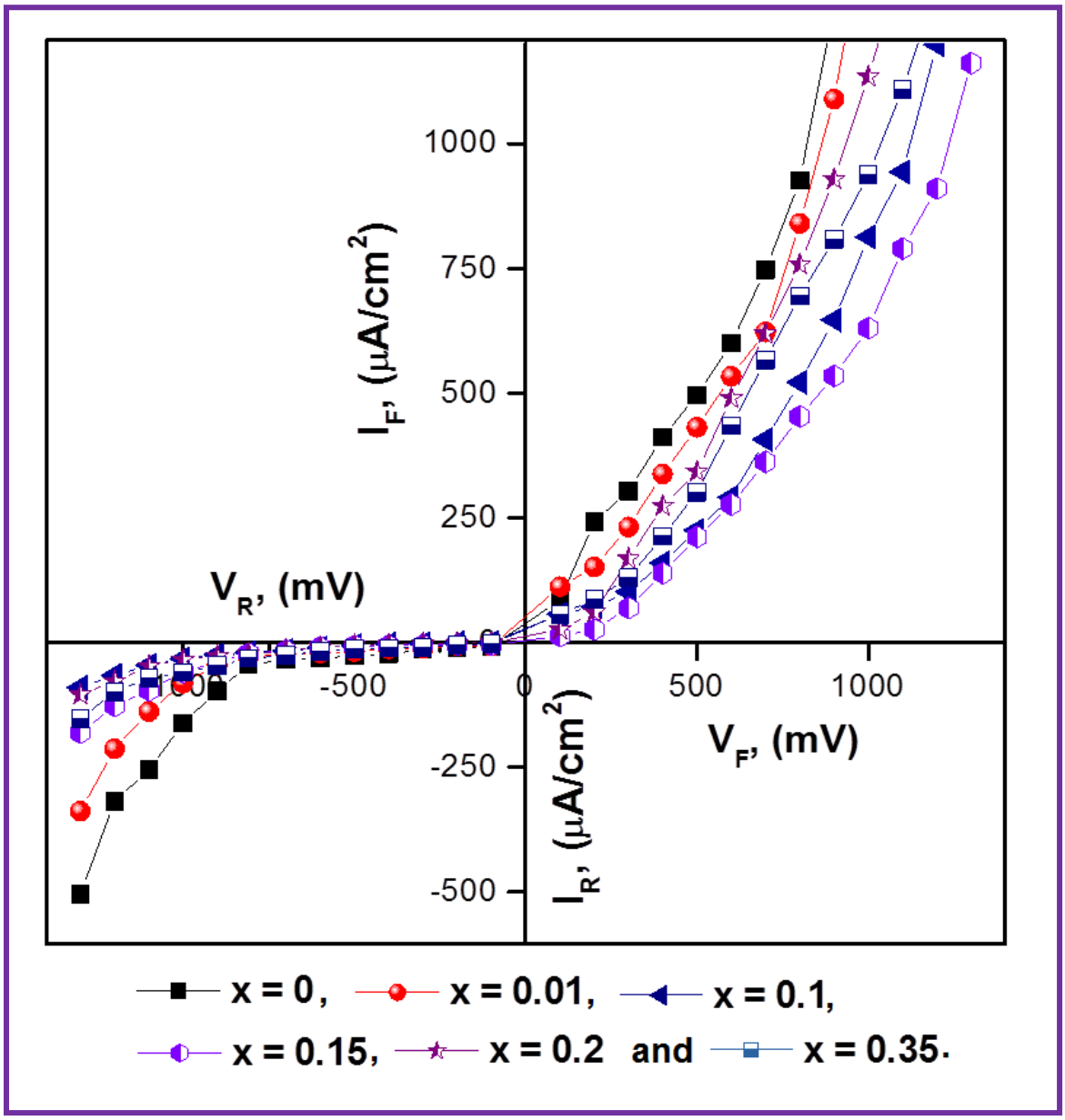

Figure 6.6. The current-voltage characteristics of the electrochemical PV-cells formed with the photoelectrodes of different compositions (x) (in dark).

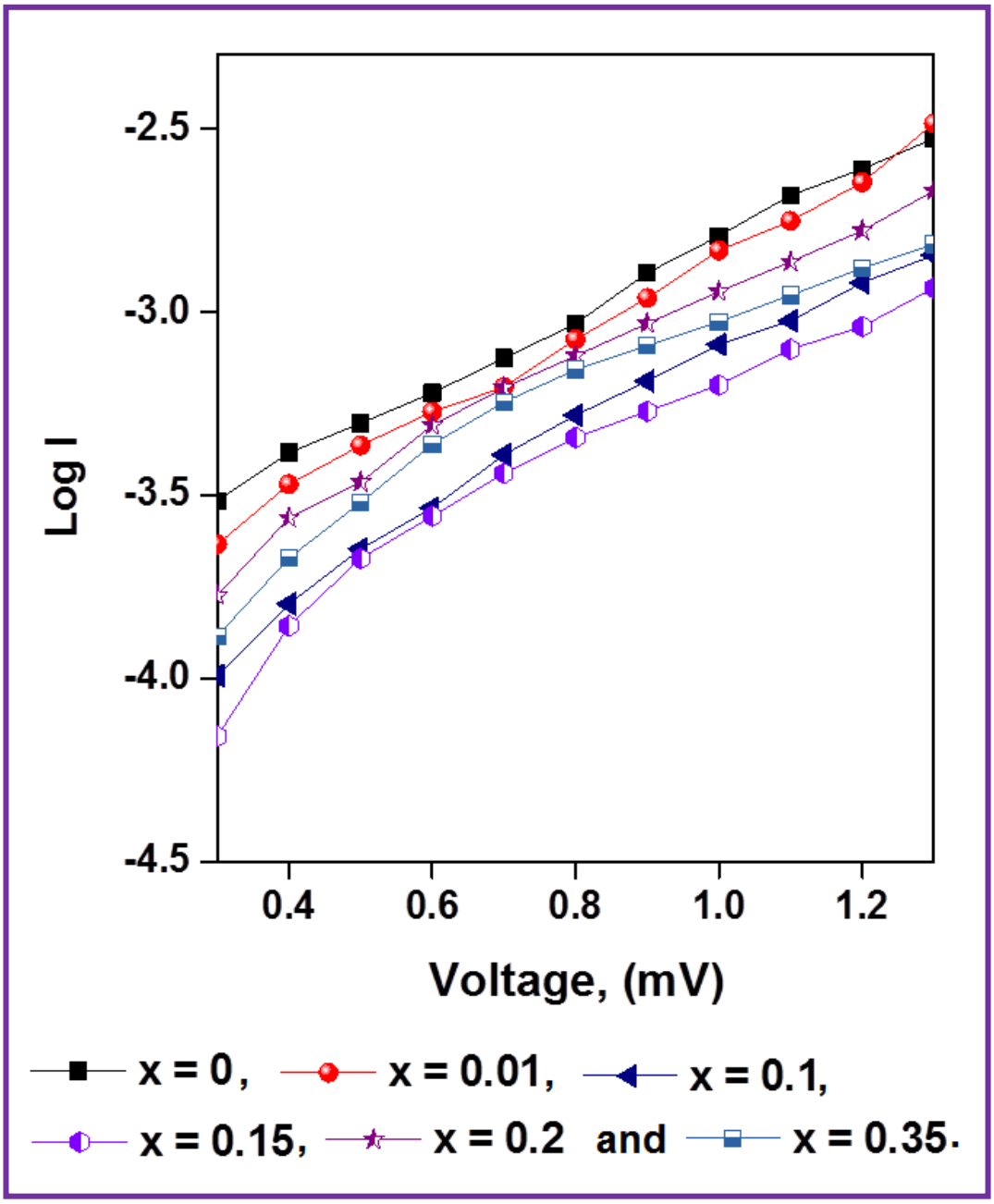

Figure 6.7. Plots of log I versus V for different PV- cells.

b) C-V characteristics in dark

The C-V characteristics of a junction provides useful information such as type of conductivity, values of the flat band potential (V_{fb}), donor density, band bending,

depletion layer width, position of the band edges, etc. The flat band potential (V_{fb}) of a semiconductor gives information about the relative positions of the Fermi levels in the photoelectrode as well as in the electrolyte and the charge transfer process across the junction. The intrinsic band bending at the interface is used to determine the ability of the photoelectrode to operate under short circuit condition. This is also useful to measure the maximum open circuit voltage (V_{oc}) that can be obtained from a PV-cell. The V_{fb} can be determined from the Mott-Schottky relation as;

$$\frac{1}{C^2} = \left[\frac{2}{q\varepsilon\varepsilon_0 N_D}\right]\left(\frac{V - V_{fb} - kT}{q}\right) \qquad \text{.....(6.27)}$$

where, C is the space charge layer capacitance per unit area, q is the electronic charge, ε_s is the dielectric constant of a semiconductor, ε_0 is the permittivity of the free space (8.86×10^{-14}), V_{fb} is the flat band potential, N_d is the donor density, k is the Boltzmann's constant and T is the absolute temperature.

The space charge layer capacitance was measured under reverse biased condition and the flat band potentials were obtained for all the cells. The variation of C^{-2} with voltage (vs SCE) for six representative samples is shown in fig 6.8. The linear regions of these plots were extrapolated to the voltage axis, which gave the flat band potentials (V_{fb}). The sign of the flat band potential indicates the type of the material. In this investigation, it can be concluded that $Co_{1-x}Zn_xS$ material with varying composition (x) is of the n-type. The variation of the flat band potential with composition (x) is displayed in fig.6.9. It is observed that the flat band potential is declined continuously to a less negative value as zinc content in the electrode is increased upto x = 0.4. This may

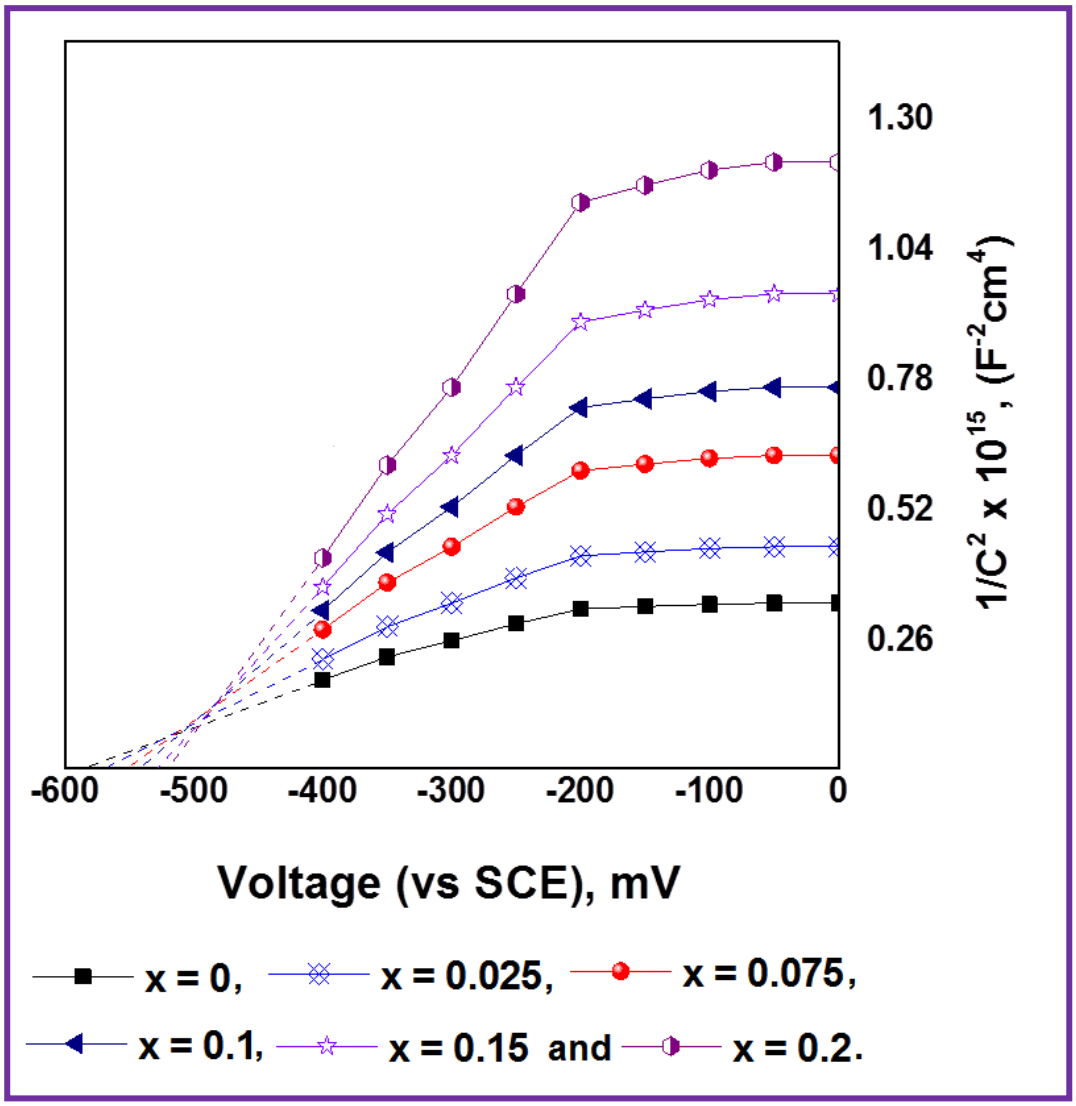

Figure 6.8. Variation of C^{-2} vs. V for all the PV- cells to determine the flat band potential, V_{fb}.

be due to: (i) decreased electron affinity as a result of introduction of Zn^{+2} ions in the lattice of CoS, (ii) an increased amount of surface adsorption and creation of a large number of surface states at the interface causing a severe Fermi level pinning and thus decreasing the amount of band bending [3, 4, 6, 12, 13, 22]. From the fig.6.8 it is also seen that the plots diverge from linearity when the electrode voltage becomes less

negative which is an indicative of the fact that junctions are of the graded type [4-6, 12, 22]. This type of behaviour has also been observed previously and is attributed to the presence of surface states at the interface that decreases the electrochemical performance [5, 6, 12, 22].

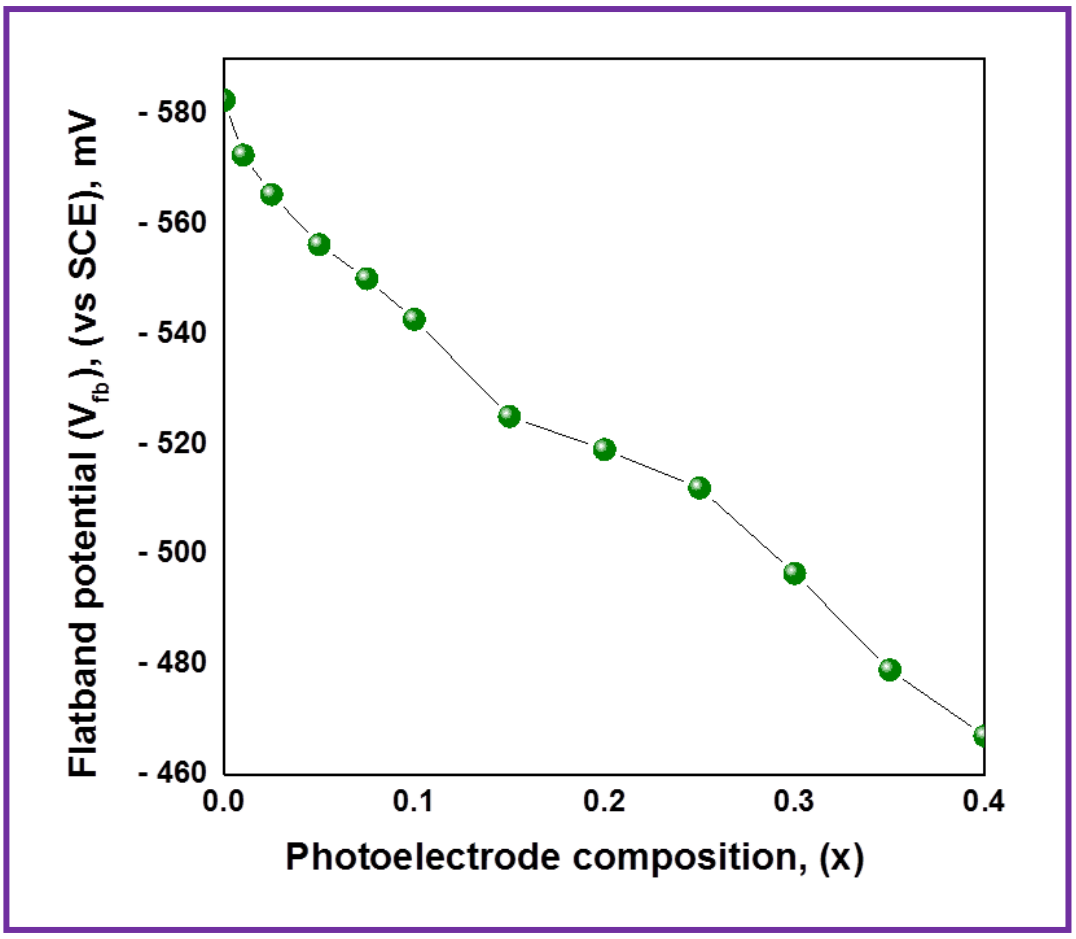

Figure 6.9. A plot of V_{fb} vs. composition parameter (x).

c) Built-in-potential measurements

The built-in-potentials (also called barrier-height, Φ_{β}) were determined by measuring the reverse saturation current (I_o) flowing through junction at different temperatures from

303 K to 363 K. The reverse saturation current flowing through the junction is related to the temperature as [3, 4, 12];

$$I_0 = AT^2 \exp\left(\phi_\beta / kT\right). \qquad \text{.....(6.28)}$$

where, A is a Richardson constant, k is a Boltzmann constant and Φ_β is the barrier height in eV. The reverse saturation current exhibits an almost exponential variation with temperature. Fig. 6.10 shows plots of log (I_o/T^2) versus 1000/T for eight representative cells. The values of the built in potentials of the various PV-cells were then determined

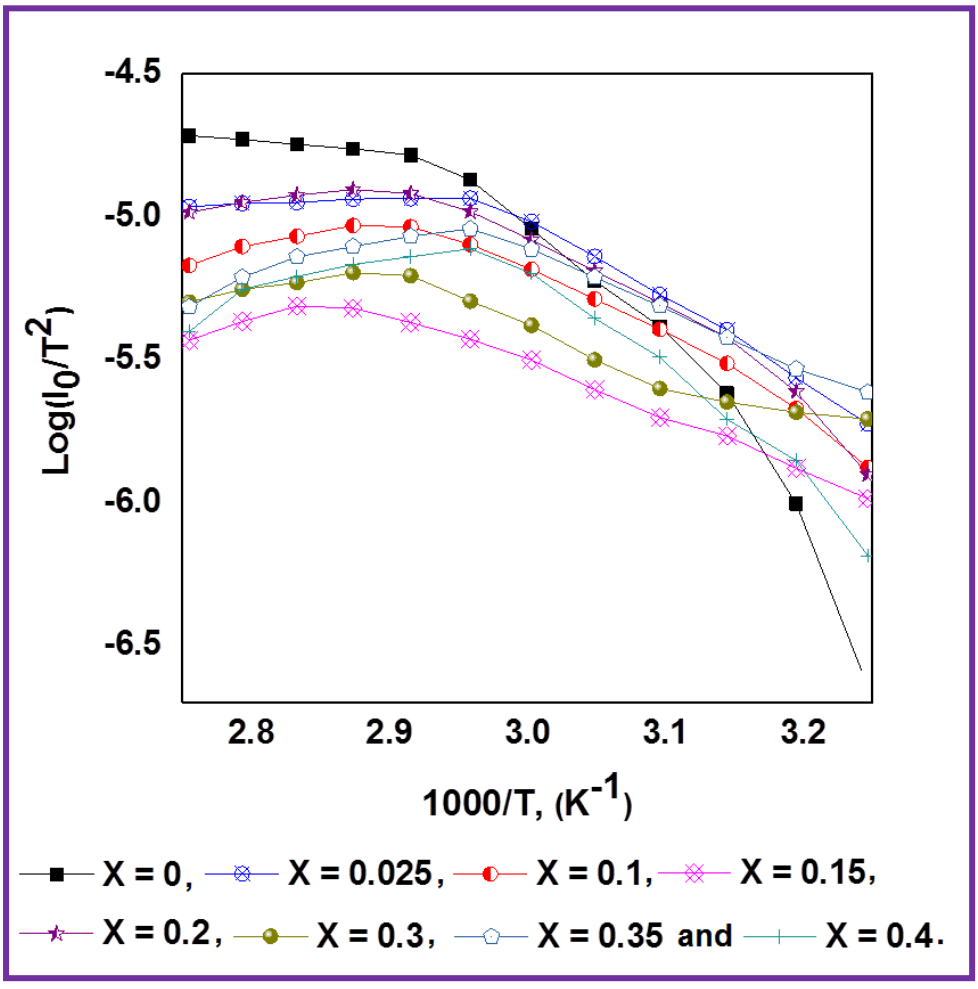

Figure 6.10. Typical plots of log (Io/T^2) with 1000/T for various cells.

from the slopes of the linear regions of the plots and are documented in table 6.2. Further, it is also notable that the plots tend to be nonlinear at high temperatures and can be attributed to the Pool-Frenkel type conduction mechanism [3, 4, 12]. The built-in-potential is found to be bit increased with x and then decreased, but has no systematic variation. The increase and decrease in Φ_β can be explained as usual.

d) Power output characteristics

When the PV cell is illuminated by a light of constant illumination intensity, the I-V characteristics shifts in fourth quadrant which is in accordance with the usual theory of the solar cell as an electricity generator. The excess charge carriers generated as a result of the photon absorption in the active region of the electrode / electrolyte interface are separated; electrons move deep into bulk, while holes move to the surface of the semiconductor electrode. The charge separation process continues until it results in a counter field, which is maximum at the open circuit condition, called the open circuit photo potential (V_{ph}). In the present case, power output curves were obtained for the cells at a fixed input intensity of 25 mW/cm^2.

Fig.6.11 shows the power output curves. The cell characteristics namely, open circuit voltage (V_{oc}), short circuit current (I_{sc}), efficiency (η %), fill factor (ff), series resistance (R_s) and shunt resistance (R_{sh}) were then computed from these curves and are listed in table 6.2. It is seen that V_{oc} has a maximum value of 404 mV for a cell formed with CoS electrode and decreased thereafter. The variations in I_{sc} and V_{oc} with x are not systematic and the observed variations are due to the light absorption and the cell series

resistance (R_s) effects. The other cell performance parameters were calculated and are cited in table 6.2.

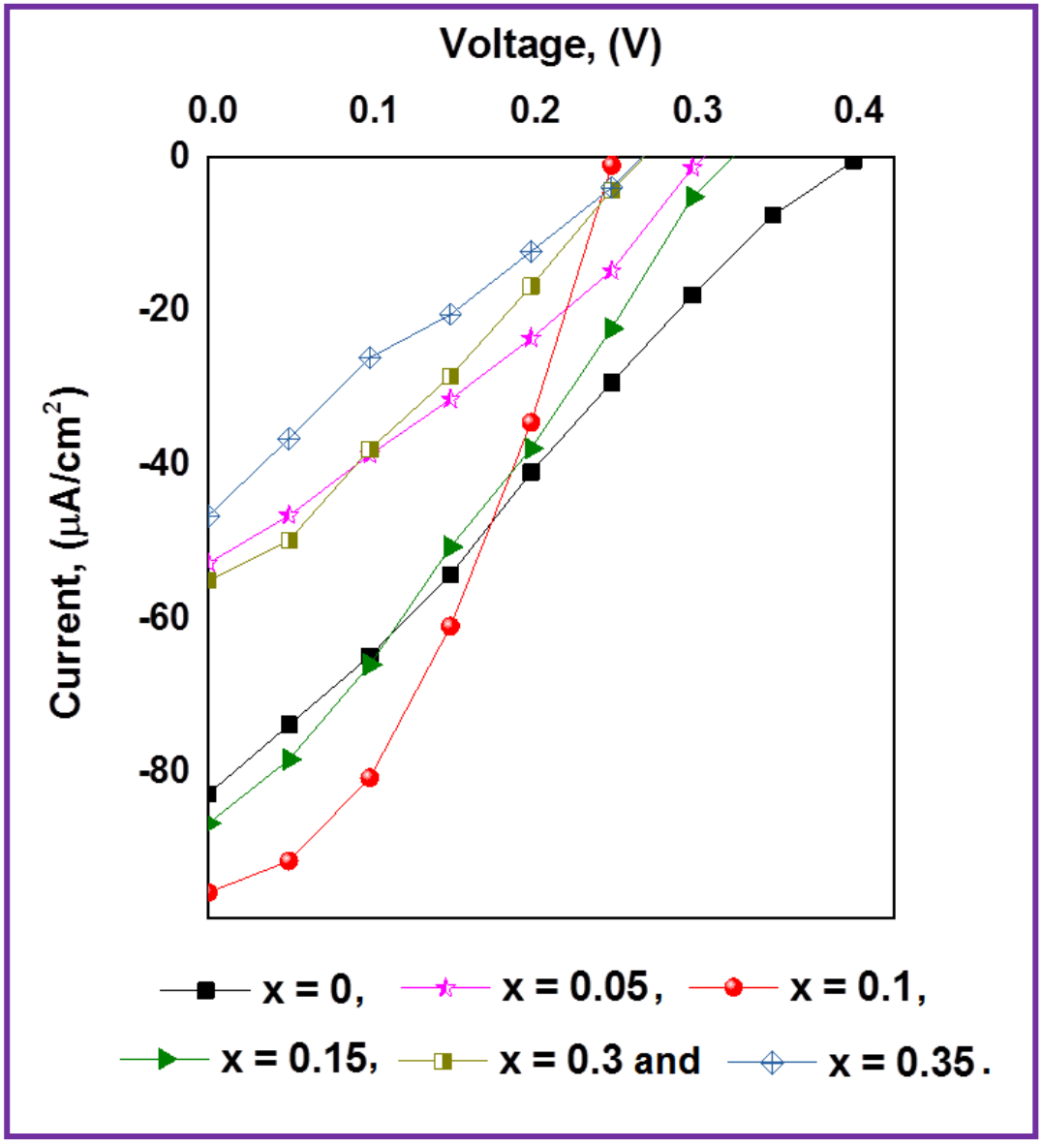

Figure 6.11. Power output curves for various PV-cells comprising various electrode compositions (x).

The other parameters are efficiency (η %), fill factor (ff %) series and shunt resistances (R_s and R_{sh}), etc. and their variations are shown in table 6.2. The closer inspection of table 6.2 shows that, the results are unsystematic and the PV-performance is not satisfactory. Similar results have been reported by Lue and Kamat [23] that the photogenerated charge carriers may move in both the directions causing significant leakage into the electrolyte itself, instead of flowing through the external circuit. In the present studies, all the fabrication parameters and conditions were kept at their optimum values and only electrode composition was varied. Therefore, our observations in the PV-performance are solely due to the changes in the electrode properties due to the incorporation of Zn into CoS. Much is required to be done to change the properties of the electrode material in tune with the electrolyte properties. Further, search for other matchable electrolyte is also a stringent requirement.

6.4.3. Studies on the optical proprieties of the PV cell

The optical properties namely, photo, speed and spectral responses were also investigated. Fig(s). 6.12 and 6.13 show the action spectra and transient responses of the various cells, respectively. From the action spectra, it is seen that the $Co_{1-x}Zn_xS$ material is spectrally less sensitive within the range of wavelengths studied. In actual, material should show peak performance in the certain range of incident wavelengths showing its sensitivity to the incident radiations. Fig. 6.13 shows the speed/ transient responses of the various PV-cells. Both rise and decay of V_{oc} with time are shown. These observations also show a large amount of surface states at the interface. The rise and

decay of V_{oc} with time should be faster indicating least amount of surface states at the interface. However, present studies show a very large concentration of surface states at the interface showing unsystematic and discouraging status (present) of the material as a PV-material.

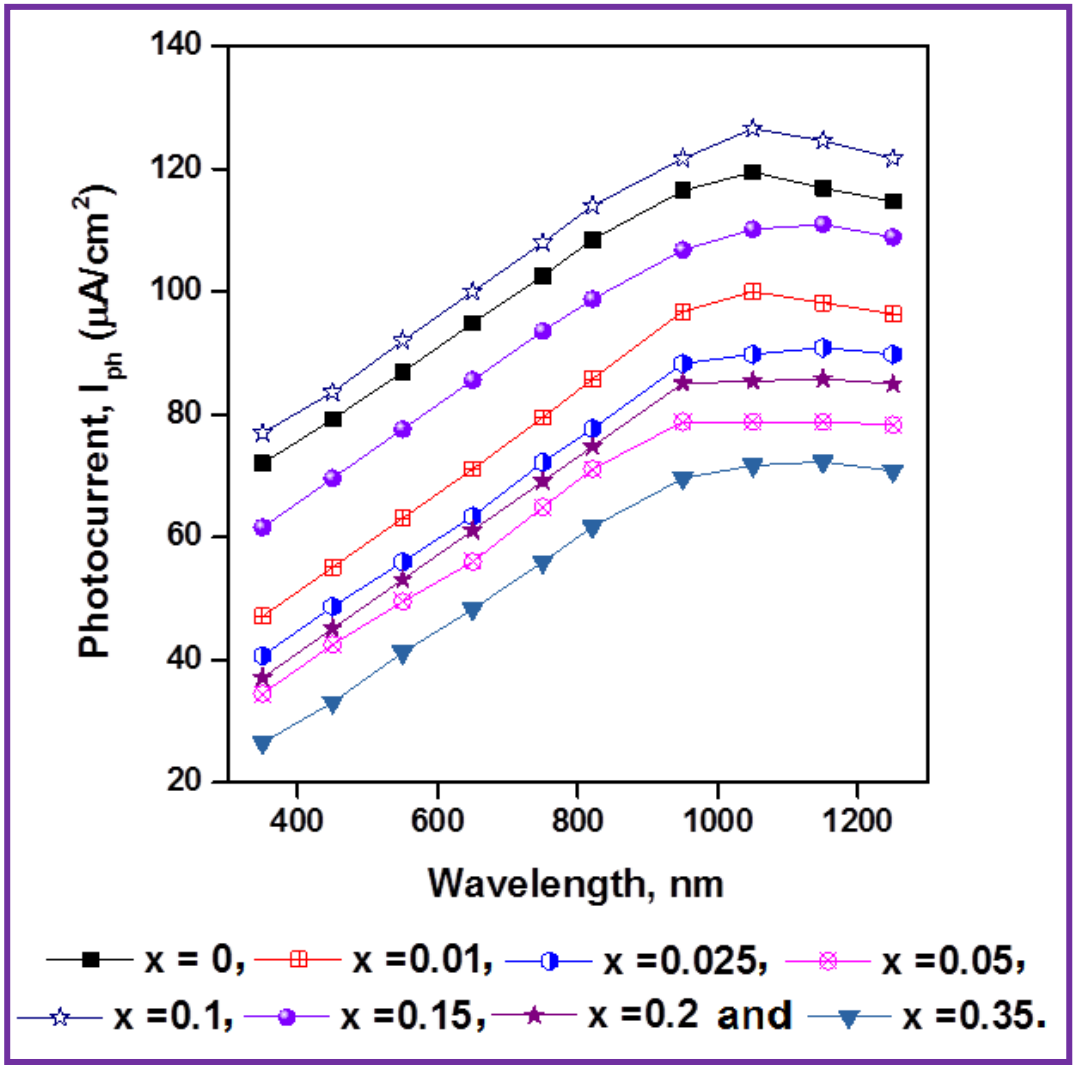

Figure 6.12. The action spectra for various cells formed with the CoS and $Co_{1-x}Zn_xS$ photoelectrodes.

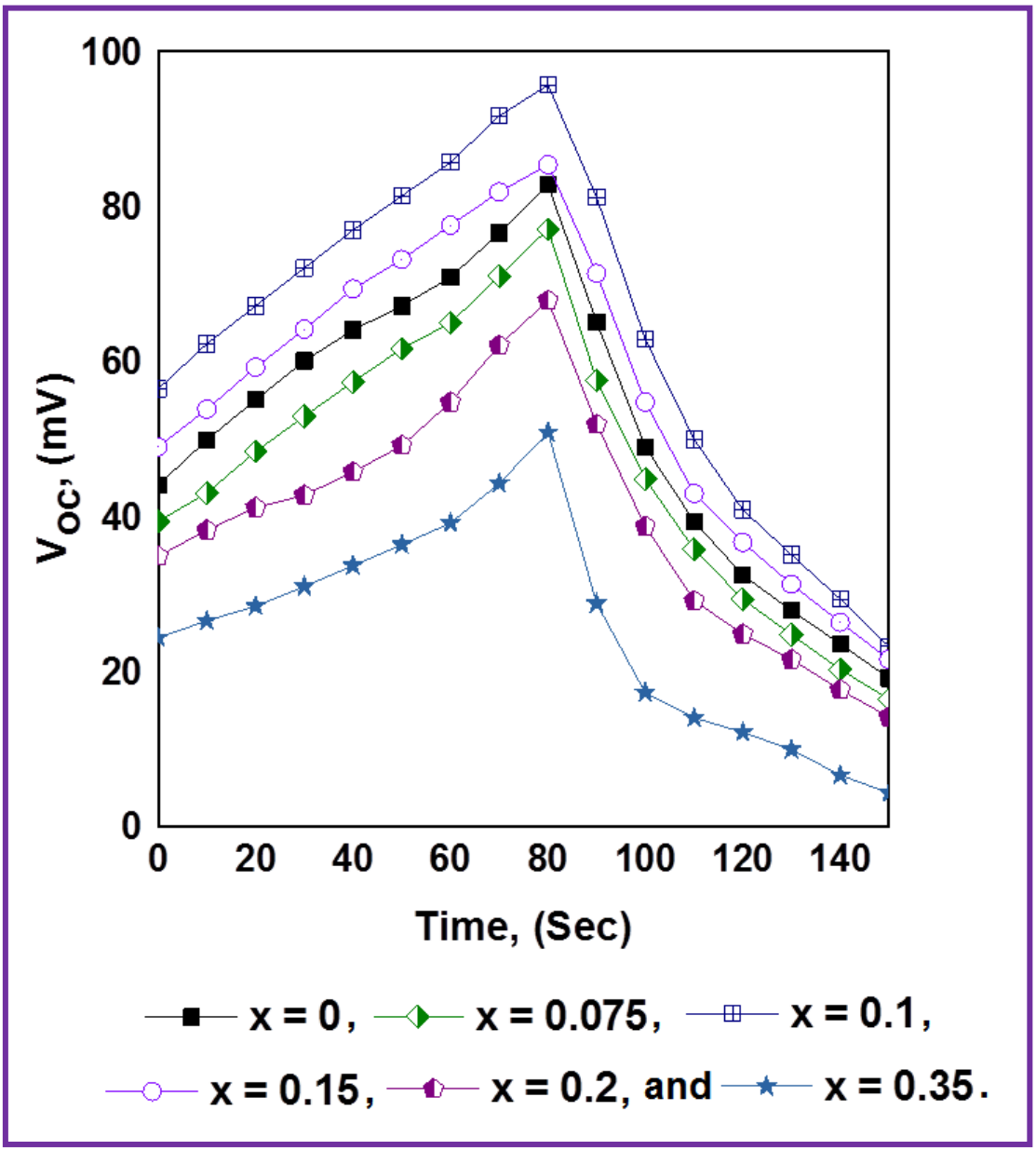

Figure. 6.13. Rise and decay of V_{oc} with time for the PV cells.

6.5. Conclusions

1. A solid-liquid junction electrochemical photovoltaic cell is devised with CoS and $Co_{1-x}Zn_xS$ electrodes, KCl as electrolyte and graphite rod as a counter electrode. A saturated calomel electrode was used as reference electrode.
2. The cell structures were formed and behaviour of these cells was examined with a special emphasis given to the photoelectrode composition.
3. The dark I-V and C-V characteristics showed presence of the recombination centers and surface states at the electrode/electrolyte interface.
4. The efficiency is low compared to the solid state devices and needs improvement in both electrode and electrolyte properties.
5. The as-devised cell performance under light excitation is found to be optimum for a cell formed with a photoelectrode of composition $x = 0$.
6. In general, the PV- performance of a material as an electrochemical PV-cell is not observed as per the expectation.

Table 6.1. Studies showing choice of an electrolyte redox couple for CoS and $Co_xZn_{1-x}S$ ($0 \leq x \leq 0.4$) electrodes.

	Conc^n	X = 0				X = 0.15			
		I_d ($\mu A/cm^2$)	V_d (mv)	I_{sc} ($\mu A/cm^2$)	V_{oc} (mv)	I_d ($\mu A/cm^2$)	V_d (mv)	I_{sc} ($\mu A/cm^2$)	V_{oc} (mv)
KCl	**0.25 M**	37.7	244	164.6	331	101	231	119.5	251
	0.5 M	68	330	216.7	340	160	286	117.6	282
	1 M	96	456	273.1	411	209	354	236	299
	1.5 M	140	250	160.2	300	240	326	196	250
	2 M	**Electrode Corrosion**							
	3 M								
Hydroquinone	**0.25 M**	0.75	26	1.52	50	0.98	52.3	1.98	66.9
	0.5 M	1.56	45	2.16	72.3	0.76	45.8	1.45	61.8
	1 M	0.85	39	1.63	69.34	0.59	50.4	1.32	66.3
Sulphide / Polysulfide	**Electrode Dissolution**								
NH_4Cl									
DMSO									
Iodite / Polyiodite									
H_2So_4									

Table 6.2. Performance parameters of the electrochemical PV- cells of different photoelectrode composition (x).

Composition (X)	V_{oc} (mV)	I_{sc} (μA/cm^2)	R_{sh} (Ω)	R_s (Ω)	η %	ff	n_d	φ_B (eV)	V_{fb} (mV)	λ (nm)	Responsivity R, (μA/mW)
0	404.2	82.93	206	237	0.33	0.25	6.62	0.21	-582	1050	0.283
0.01	308.7	72.25	206	259	0.25	0.28	6.07	0.33	-572	1050	0.214
0.025	309.4	62.47	192	216	0.21	0.27	5.20	0.39	-565	954	0.158
0.05	305.9	52.70	144	222	0.19	0.29	4.55	0.26	-556	951	0.144
0.075	212.5	77.27	260	202	0.21	0.33	6.07	0.38	-550	1049	0.181
0.1	251.2	96.13	223	668	0.33	0.34	6.07	0.45	-543	1050	0.280
0.15	325.5	86.79	240	327	0.31	0.27	4.86	0.62	-525	1150	0.284
0.2	171.8	62.47	122	467	0.14	0.32	5.20	0.35	-519	951	0.106
0.25	326.3	60.26	159	231	0.22	0.27	5.60	0.25	-512	949	0.165
0.3	270.8	55.23	171	242	0.16	0.27	6.07	0.45	-497	1149	0.152
0.35	270.1	47.22	205	165	0.12	0.23	6.07	0.57	-479	1050	0.098
0.4	149.3	59.08	174	508	0.11	0.31	6.62	0.28	-467	1053	0.094

References

[1] B. Dimmer, H.W. Schock, Prog Photovolt Res Appl 6 (1998) 193.

[2] N. Gocsen, J .J. Loferski, Sol Energy Mater 1 (1979) 271.

[3] M. Sharon, Photoelectrochemical Solar Cells, (Eds.) K.S.V. Santhanam, M. Sharon UNESCO Training Workshop, (1986).

[4] S. Chandra, Photoelectrochemical solar cells, (Eds.), D.S. Campbell, Garden & Breach Science Publishers, N.Y. (1985).

[5] L.P. Deshmukh, S.S. Holikatti, J Phys D: Appl Phys 27 (1994) 1786.

[6] R.V. Suryavanshi, Ph.D Thesis (2013), Swami Ramanand Teerth Marathwada University, Nanded, M.S, India

[7] W. Bloss, F. Pfisterer, M. Schubert, T. Walter, Prog Photovolt Res Appl. 3 (1995) 3.

[8] J.R. Sites, T. Nakada, H.W. Schock, S. Niki, A. Yamada, M.A. Contreras, in "CIS-21 Collaboration, "Research and Development of High Voltage CIS-Based Thin Film Solar Cells for Industrial Technology", 2002 EA 007, USA (2002-2005).

[9] H. Neumann, Solar Cells 16 (1986) 317.

[10] D. Wei, G. Amaratunga, Int J Electrochem Sci 2 (2007) 897.

[11] H.Y. Liu, Ph.D. Thesis (1998), Shanghai Institute of Optics & Fine Mechanics, Chinese Academy of Sciences, China.

[12] L.P. Deshmukh, Ph.D. Thesis (1985), Shivaji University, Kolhapur, M.S, India.

[13] H. Gerischer, Topics in Applied Physics, Solar Energy Conversion, (Eds.), B.O. Seraphin, Berlin: Springer, Heidelberg, 31 (1997) 115.

[14] S.S. Kamble, Andrzej Sikora, S.T. Pawar, N.N. Maldar, L.P. Deshmukh, J Alloys Compd 623 (2015) 466.

[15] S.S. Kamble, A. Sikora, S.T. Pawar, R.C. Kambale, N.N. Maldar, L.P. Deshmukh, J Alloys Compd 631 (2015) 303.

[16] S.S. Kamble, A. Sikora, S.T. Pawar, G.T. Chavan, N.N. Maldar, L.P. Deshmukh, Some Investigations on $Zn_xCo_{1-x}S$ DMS Thin Films: Chemical Synthesis and Characteristic Properties, 2nd International Symposium on Physics and Technology of Sensors (ISPTS-2), 08–10 March 2015, Pune, India.

[17] S.T. Mane, P.C. Pingale, S.A. Lendave, V.S. Karande, L.P. Deshmukh, M. Sharon, Electrochim Acta 102 (2013) 113.

[18] S.T. Mane, P.C. Pingale, R.V. Suryawanshi, V.S. Karande, L.P. Deshmukh, M. Sharon, Electrochim Acta 114 (2013) 494.

[19] A.N. Chattarki, N.N. Maldar, L.P. Deshmukh, J Alloys Compd 597 (2014) 223.

[20] A.M.A. Dhafiri, A.A.I. Al-Bassam, Sol Ener Mater Sol Cells 33(1994) 177.

[21] P.K. Mahapartra, A.R. Dubey, Sol Ener Mater Sol Cells 32 (1994) 29.

[22] A. Aruchamy, G. Aravamudan, G.V.S. Rao, Bull Mater Sci 4 (1982) 483.

[23] D. Lue, P. Kamat, J Phys Chem 97 (1993) 1073.